



Molecular Crystals and Liquid Crystals Incorporating Nonlinear Optics

Publication details, including instructions for authors and
subscription information:

<http://www.tandfonline.com/loi/gmcl17>

Slow Dynamics in a Convecting Nematic: A Neutron Scattering Study

Tormod Riste^a & Kaare Otnes^a

^a Institutt for Energiteknikk, FOB 40, N-2007, Kjeller, Norway
Version of record first published: 22 Sep 2006.

To cite this article: Tormod Riste & Kaare Otnes (1990): Slow Dynamics in a Convecting Nematic: A Neutron Scattering Study, Molecular Crystals and Liquid Crystals Incorporating Nonlinear Optics, 191:1, 109-121

To link to this article: <http://dx.doi.org/10.1080/00268949008038584>

PLEASE SCROLL DOWN FOR ARTICLE

Full terms and conditions of use: <http://www.tandfonline.com/page/terms-and-conditions>

This article may be used for research, teaching, and private study purposes. Any substantial or systematic reproduction, redistribution, reselling, loan, sub-licensing, systematic supply, or distribution in any form to anyone is expressly forbidden.

The publisher does not give any warranty express or implied or make any representation that the contents will be complete or accurate or up to date. The accuracy of any instructions, formulae, and drug doses should be independently verified with primary sources. The publisher shall not be liable for any loss, actions, claims, proceedings, demand, or costs or damages whatsoever or howsoever caused arising directly or indirectly in connection with or arising out of the use of this material.

SLOW DYNAMICS IN A CONVECTING NEMATIC: A NEUTRON SCATTERING STUDY

TORMOD RISTE AND KAARE OTNES

Institutt for Energiteknikk, POB 40, N-2007 Kjeller, Norway

Abstract Nematic PAA, exposed to a vertical temperature difference ΔT , exhibits oscillatory convection whose frequency ω can be measured by real-time neutron scattering. We have studied the soft-mode character and the physical origin of the phenomenon, and discuss their relation to phenomena at equilibrium phase transitions.

The Fourier components of the observed power spectrum reveal a change of the flow pattern at increasing ΔT that can be compared with predictions from hydrodynamics and with theories of chaos.

Finally we have studied the decreasing slope of the soft mode (defined as $\omega^2/\Delta T$) as the mean temperature of the sample is approaching the supercooling limit.

INTRODUCTION

Liquid crystals provide us with a rich laboratory for experiments in various fields of physics. In the present paper we intend to demonstrate that in a single experimental setup, usually associated with hydrodynamics, we may also study problems of current interest in statistical physics and in condensed matter physics.

The phenomenon that we study is thermal convection. This ubiquitous, natural phenomenon has obtained renewed interest in recent years, because of the possibility it offers for studying the development of chaos and turbulence. Usually convective flow starts as a regular, stationary pattern of convection rolls. At higher values of the control parameter, the applied vertical temperature difference ΔT , a time-periodic regime is observed. A well-known route towards turbulence (i.e. temporal chaos), is the perioddoubling route in which the power spectrum develops a cascade of subharmonics. At still higher values of ΔT turbulence manifests itself as a quasi-continuous chaotic spectrum.

Theory and experiments on convection in nematic liquid crystals were pioneered by the Orsay group. Lekkerkerker¹, followed by others^{2,6}, showed theoretically that oscillatory time periodic flow is to be expected in nematics with a vertically aligned director. Guyon et al. subsequently verified this prediction, using induced oscillations. Oscillatory convection is expected for any double-diffusive system, in liquid crystals Lekkerkerker¹ ascribed this property to relaxation of

temperature and orientation.

In a series of papers⁸⁻¹² we, together with Möller, have reported on studies of thermal convection in nematic para-azoxyanisole by neutron scattering. Already in 1975⁸ we made the first observation of oscillatory convection, at the dawn of the resurgent interest in chaotic phenomena. Later we have reported on the unexpected soft-mode behaviour of the oscillatory frequency⁹, on the multistability property of the convection pattern¹⁰ and on the phase coupling of localized oscillators¹¹. Very recently we have observed spatiotemporal Fourier components of the flow¹². The present paper is a review of these phenomena, with an emphasis on the latest observations.

2 THEORY

Convection¹ is usually described in the space of the dimensionless variables R and P . For an isotropic liquid the Rayleigh number R is defined as

$$R = \frac{\alpha g \Delta T d^3}{\kappa \nu} \quad (1)$$

α : thermal expansion coefficient
 g : acceleration of gravity
 d : depth of the liquid
 κ : thermal diffusivity
 ν : kinematic viscosity

P , the Prandtl number is defined as

$$P = \frac{\nu}{\kappa} \quad (2)$$

Liquid crystals are anisotropic liquids, and the expressions for R and P have to be modified by the introduction of the anisotropic transport coefficients.

Independent of P , the onset of convection occurs at the threshold value $R_c = 1707$. This numerical value is valid for a liquid container of infinite aspect ratio, i.e. width-to-depth ratio. For small aspect ratios R_c will be higher¹⁴.

For a low-Prandtl number fluid Busse¹⁵ predicted that the first oscillatory instability in Rayleigh-Bénard convection consists of a wavy motion along the horizontal roll axis. For the frequency he gave the formula

$$\omega \propto \tau_{th}^{-1} q \left(\frac{\Delta T - \Delta T_c}{\Delta T_c} \right)^{1/2} \quad (3)$$

$\tau_{th} = d^2/\kappa$ is the thermal relaxation time and q is the wave number. Busse has also given a complete stability diagram with phase boundaries for the periodic and higher instabilities¹⁶. The result is the so-called Busse balloon in (R, P, q) -space. A cut through the balloon at constant P gives a curve whose bottom part is the marginal stability curve

$$(R-R_c) \propto (q-q_c)^2 \quad (4)$$

The wave number of the rolls at the onset of convection $q_c = \pi/d$, i.e. the diameter of the roll fits the depth of the fluid layer. Smaller rolls are excited at higher values of R .

In the introduction above we made no distinction between chaos and turbulence. Heslot & al.¹⁷ have recently introduced the classification in which chaos involves a disordered time behaviour but a coherent spatial structure. Spatial coherence is only lost in the fully turbulent regime, at very high ($> 10^8$) values of R .

The theories for liquid crystals³⁻⁵ predict the oscillatory convective state to bifurcate from the stationary convective state with a frequency

$$\omega \propto (\tau_{th}^a \tau_{th})^{-1/2} \quad (5)$$

in which τ_{th}^a denotes the anisotropic part of τ_{th} . This oscillatory convection should only occur in a nematic with a vertically aligned director, and the frequency should depend markedly on H . The theories just referred to ascribe oscillatory convection in a nematic to the double diffusive property of the substance, i.e. the existence of two (or more) relaxational mechanism. Nematics share this property with two-component liquids, thermo-haline liquids etc.

3. EXPERIMENTS

A sketch of the experimental setup is given in Fig. 1. Entrance slits of different sizes may be inserted for definition of the area of the irradiated sample. The sample cell is made of aluminum with very thin

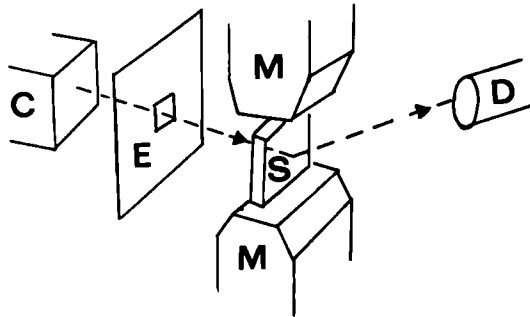


FIGURE 1. Sketch of the experimental setup. C is the exit collimator of the neutron beam channel, E an entrance slit with an expandable and movable opening, S the aluminum sample container (inner dimensions 30x30x3 mm), M a magnet and D the neutron detector. Not shown are heating elements on bottom and top of S that maintain an adjustable temperature difference ΔT .

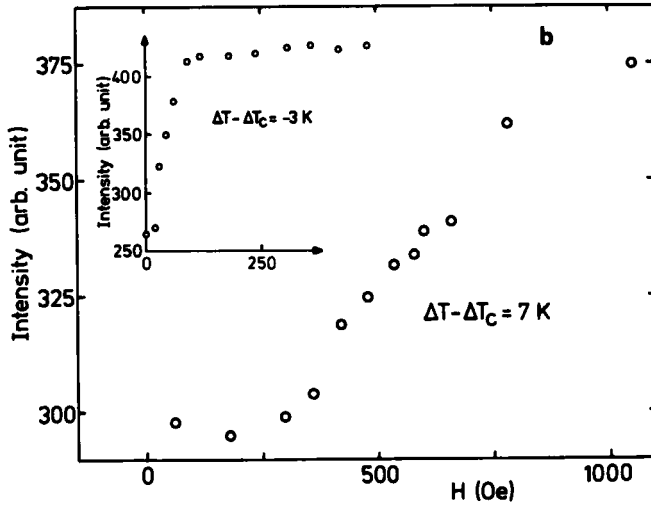


FIGURE 2. Neutron intensity versus applied magnetic field. An inset shows the same for $\Delta T < \Delta T_c$, i.e. in the absence of flow.

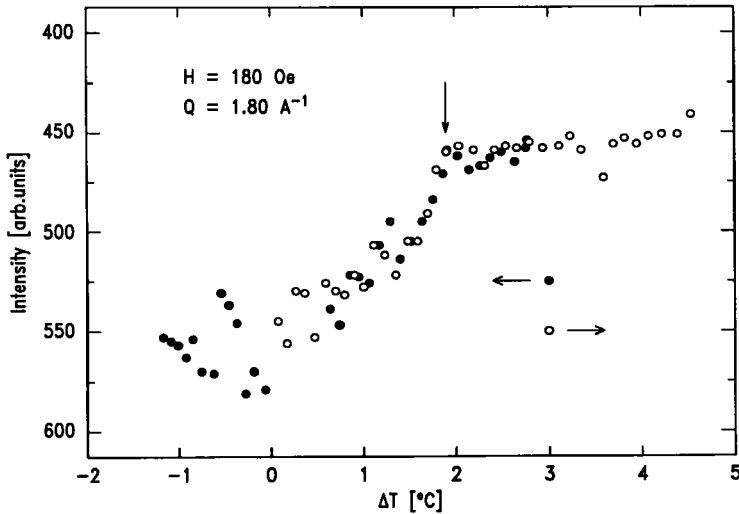


FIGURE 3. Neutron intensity versus ΔT , the vertical temperature difference. The convection threshold is marked by a vertical arrow.

side-walls. Heating elements in the bottom and top lids enable the temperatures and temperature differences to be kept constant within $\sim 0.01^\circ$. The geometrical shape of the cell is suitable for a neutron scattering experiment, and is of the Hele-Shaw type. For the given geometry (aspect ratios) $T_c \sim 7 \cdot 10^\circ$.

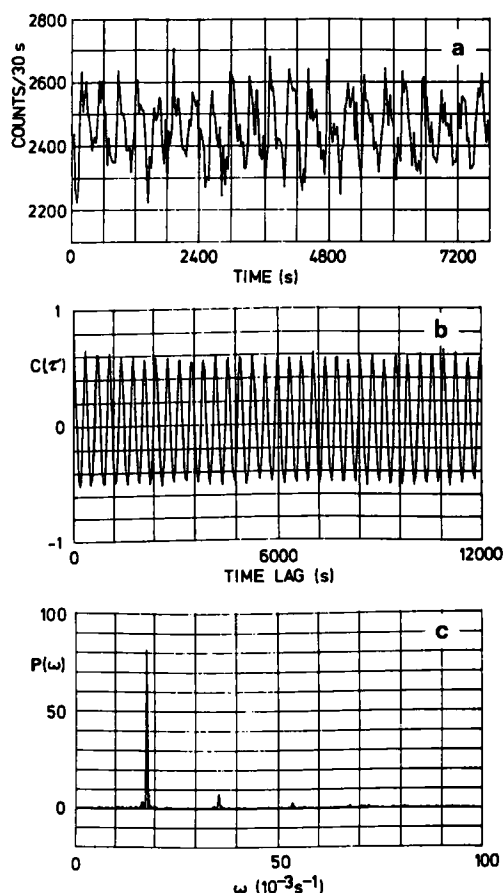


FIGURE 4a-c. An example of raw and processed data: **a** a portion of recorded neutron intensity versus time $I(t)$; **b** autocorrelation function $C(\tau) = \langle I(t) \cdot I(t+\tau) \rangle$, **c** power spectrum.

The liquid is fully deuterated paraoxyanisole with a melting temperature of 119° and clearing point 135° . The nematic phase was found to persist down to $T_0 = (92.5 \pm 1)^\circ \text{C}$ by slow supercooling. The intensity of the liquid diffraction peak at 1.8 \AA^{-1} depends very strongly on the director. For a vertical orientation the intensity has its maximum value, for a horizontal one the intensity (above the isotropic background) is zero. Due to the coupling between orientation and flow the convective state can be monitored from the scattered intensity.

For a sample of the given size it takes only ~ 50 Ørsted to align the director in the conductive state ($\Delta T < \Delta T_C$), as seen from the inset of Fig. 2. In the convective state ($\Delta T > \Delta T_C$) a field ~ 500 Ørsted is needed, as seen from Fig. 2. The data demonstrate the importance of avoiding convective flow in the measurement of the Fredericksz transition. The inset is only a qualitative measurement of this transition, since no precaution was taken to secure an anchoring at the sidewalls.

The onset of convection is measured in Fig. 3, which was measured at the centre of the sample with a narrow (10×20) mm² entrance slit. The shape of this curve depends on the slit width and the magnitude of the magnetic field, but an intensity change is always observed at ΔT_C ¹².

Each point in Fig. 3 represents the average intensity in a long time series. The top panel of Fig. 4 gives an example of raw data in such a time series. An oscillatory behaviour is apparent and made clearer in the autocorrelation (b) and in the power spectrum (c) of the same data. The frequency thus obtained strongly depends on ΔT , as displayed

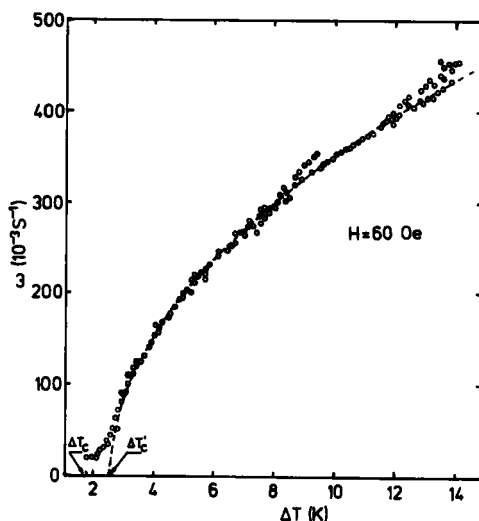


FIGURE 5. Frequency ω of oscillatory mode versus applied vertical temperature difference ΔT , as derived from data exemplified by Fig. 4. The amplitude of a function $\omega \sim (\Delta T - \Delta T_C)^{1/2}$, the broken line, is adjusted to fit the data.

in Fig. 5. The oscillatory behaviour starts at ΔT_C , measured in Fig. 3, with a finite frequency. The positions of the sidebranches, seen in Fig. 5, depend on the strength of the magnetic field (H). In Fig. 6 we have measured the frequency in the main branch, at a constant ΔT , as a function of H . An increase of ω is observed above the "Fredericksz field" of the convective state, as measured in Fig. 2.

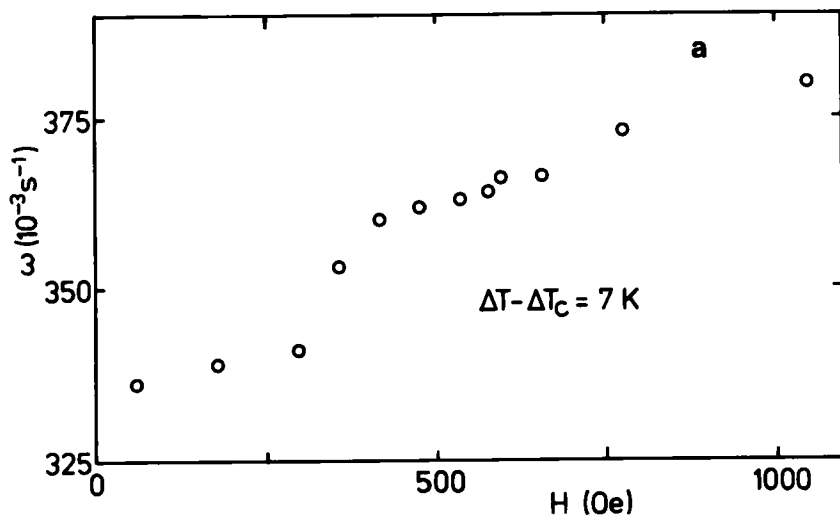


FIGURE 6. Frequency ω versus applied magnetic field H .

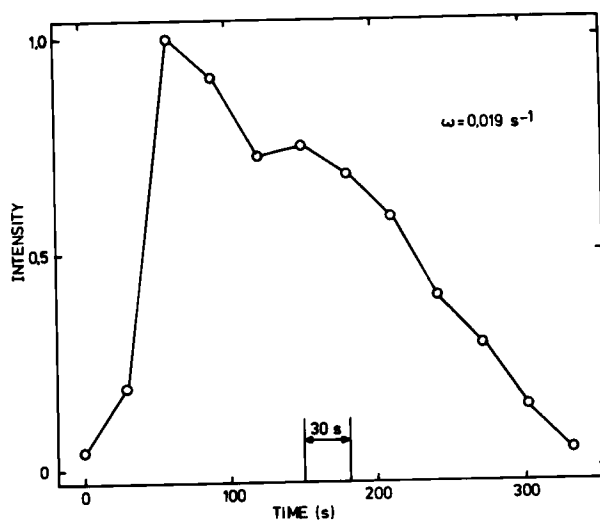


FIGURE 7. Pulse shape of Fig. 4a, after averaging over several periods. The width of the detector time channel is indicated.

An asymmetry of the oscillations, consisting of a steep front and a sloping trailing edge, is apparent already from Fig. 4a. The profile of an individual peak, as obtained by averaging over the same time series, is shown in Fig. 7. Clearly the oscillations are not linear, but relaxational and nonlinear. This is also seen in the phase portrait, an object that can be reconstructed from the time series. The portrait²⁰ reveals an object (attractor) of a dimension that is distinctly higher than that of a simple limit cycle corresponding to linear oscillations.

In a recent paper¹³ we have investigated the possible origin of the side branches seen in Fig. 5. To this end we have measured a whole set of similar curves for different values of T , the temperature of the bottom plate of the sample container. An example of such a curve is given in Fig. 8, in which the square of the frequency is plotted versus ΔT . The data have been fitted to a twodimensional (2-D) generalization of the Busse formula, equation (3). Realizing that our sample cell is quasi 2-D, we write $q = (2\pi/d)(h^2 + k^2)^{1/2}$, where (h,k) are 2-D Fourier indices. Furthermore, we allow ΔT_c to

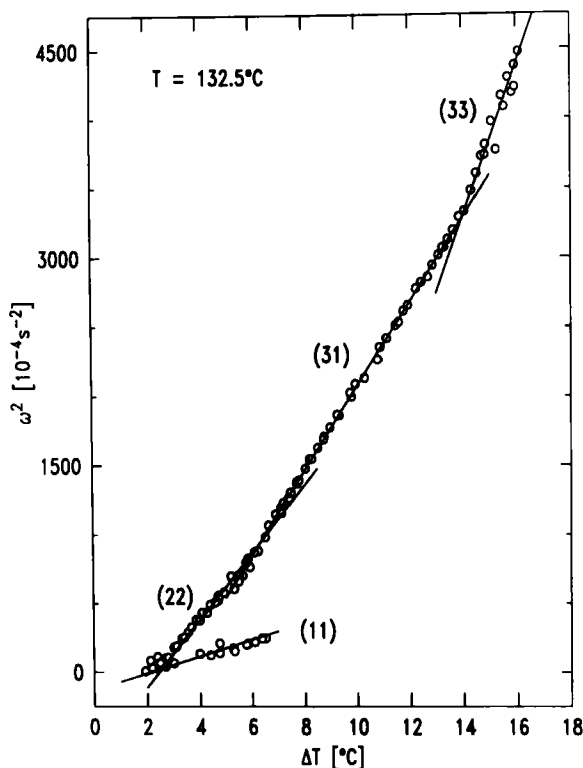


FIGURE 8. At fixed temperature $T = 132.5^\circ\text{C}$ of the bottom plate, the frequency squared reveals sequential excitations of 2-D Fourier components, as explained in the text.

depend on q , and use the notation $T_C^{(h,k)}$. This gives

$$\omega^2 \propto (h^2 + k^2)(\Delta T - \Delta T_C^{h,k}) \quad (6)$$

In Fig. 8 the line indexed by (3.1) has been least-squares fitted to the data in the range $7^\circ < \Delta T < 14^\circ \text{C}$. The slopes of the other lines are then obtained from that line, using formula (5). It is seen that the indices obey the selection rule $(h + k) = 2n$, with $n = 1, 2, \dots$, as predicted for static convection rolls in a Hele-Shaw geometry^{2†}. By extrapolating the lines to $\omega = 0$, we obtain the data points for

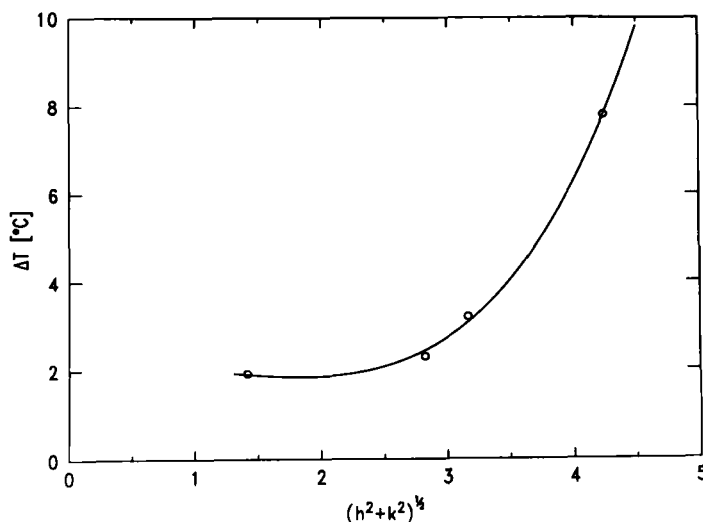


FIGURE 9. Observed data for $\Delta T_C^{(h,k)}$ versus $q = (h^2 + k^2)^{1/2}$ and least squares fit to a power expansion in $(q - (q - q_{1,1}))$.

$\Delta T_C^{(h,k)}$ shown in Fig. 9. The curve drawn is a least-squares fit to the following generalization of equation (4):

$$(\Delta T_C^q - \Delta T_C^{(1,1)}) \propto [a + b(q - q_{(1,1)})^2 + x(q - q_{(1,1)})^4] \quad (7)$$

We find that, at any value of T , the slope of $(\omega^2, \Delta T)$ can always be indexed by the same sets of (h, k) . In Fig. 10 we have plotted the slope $(\omega^2/\Delta T)$ of the (2,2)-line versus T . A least-squares fitted line to the observed points extrapolates to T_0 , the supercooling limit. In an inset we also show that $\omega^2(\Delta T_C)$, the frequency gap at the convection threshold, extrapolates to zero at $T \sim T_0$.

We have also verified, by horizontal intensity scans over the sample cell, that the spatial convection pattern can be indexed on the same 2-D lattice. The picture that appears is one of localized convection rolls that speed up and slow down in an oscillatory fashion. The next

question to ask is whether the rolls speed up and slow down at the same time, i.e. what their phase coupling is. From Fig. 11, we see that neighbouring rolls may be coupled in antiphase: with a wide entrance slit, which looks at two convection rolls, the frequency is twice of that seen with a narrow slit aiming at a single roll. At other values of ΔT we have observed phase coherence and phase incoherence.

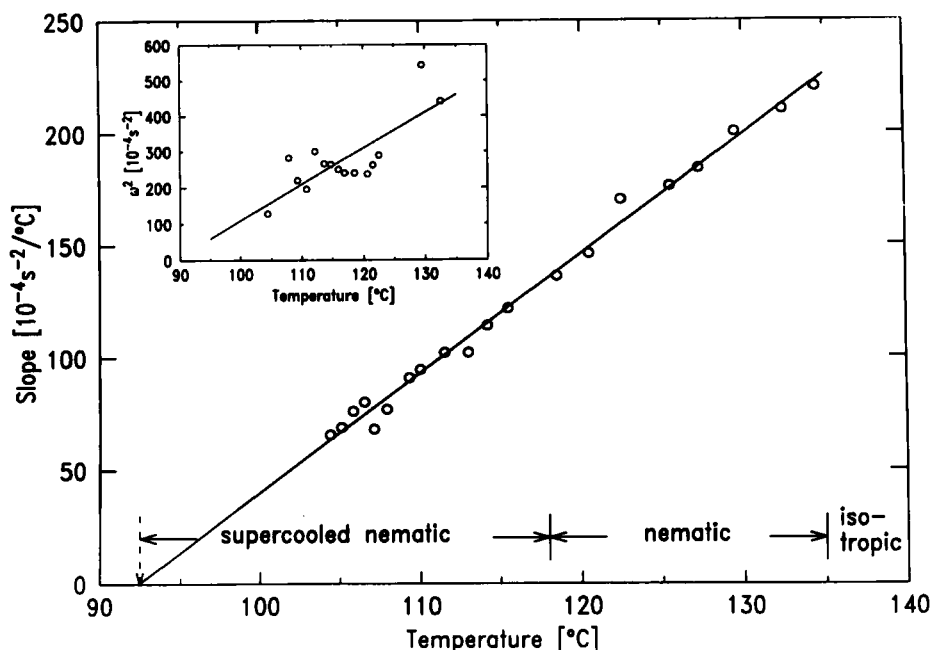


FIGURE 10. Slope of the (2,2)-line of Fig. 9 plotted versus T , the temperature of the bottom plate. The inset shows the temperature variation of the frequency gap at the convection threshold.

4. DISCUSSION

Our experiments cover a region of Rayleigh numbers extending to $\sim 5 \cdot 10^5$. In this regime the Chicago group¹⁷ finds that convection in a helium gas can be subdivided by several states termed convective, oscillatory, chaotic and transitory. If a nematic liquid crystal had the same behaviour, we should have passed through all these states and entered the soft turbulent regime at ΔT_{\max} . Our observations indicate a quite different behaviour throughout the whole regime. First of all the oscillatory state encompasses the whole convective regime. The oscillations are nonlinear and relaxational. A pattern of rolls develops that can be indexed on a two-dimensional lattice with a sel-

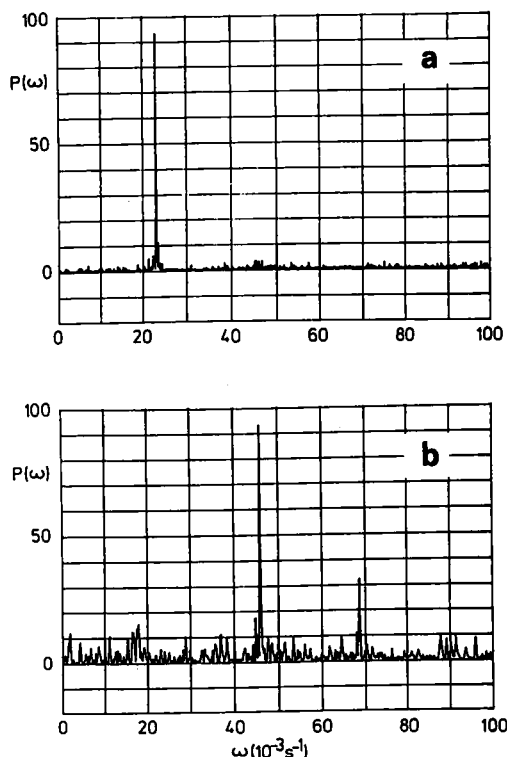


FIGURE 11. Power spectra measured with a narrow (a) and wide (b) entrance slit at a value of ΔT where localized oscillators are coupled in anti-phase.

action rule $(h + k) = 2n$. As ΔT increases there is a tendency for frequency hardening and a sequential activation of higher-index modes, see Fig. 8. At the same time the phase coupling changes from a coherent to incoherent state, a behaviour predicted by Frøyland²². This behaviour in space, time and phase can be viewed as an optimization of the convective heat transport: As ΔT increases, more channels are opened for heat flow and the flow from bottom to top becomes faster and more evenly distributed in time. It is interesting to notice that in a recent paper Beloshapkin et al.²³ predict a preturbulent region in hydrodynamic systems in which the pattern develops from crystalline to quasicrystalline. The cells of the pattern are divided by channels in which dynamical chaos develops. In our observations the phase relation between the cells in an ordered pattern plays an important role. Clearly temporal chaos may result from phase incoherence and spatial chaos from pattern competition, and experimental data from local and nonlocal measurements may look quite different.

The curve of Fig. 5 bears a strong resemblance to soft modes in equilibrium phase transitions²⁴, only that T is replaced by ΔT . The approaches to the phase transitions T_c and ΔT_c are very similar: neither of them soften to $\omega = 0$, instead an asymptotic approach to a finite frequency is observed. In the equilibrium case this critical behaviour is governed by the microscopic thermal diffusivity²⁵. Our present experiments suggest that the macroscopic, convective heat

transport has a soft-mode behaviour. So far no satisfactory theory exists for the value of the frequency that we observe. Equations (3) and (5) both relate $\omega(\Delta T_c)$ to τ_{th} , but the temperature behaviour of the frequency, as displayed in Fig. 10, seems to rule out a direct inverse proportionality to any of the actual relaxation times. In a nematic liquid crystal $\tau_{th} \propto S^{-1}$, the inverse order parameter¹⁶. The relaxation times of velocity and orientation are both dominated by the temperature behaviour of the viscosity, which would imply an essential singularity as $T \rightarrow T_g$ ²⁷. Also the response of the frequency to the applied magnetic field, see Fig. 6, is different from the theoretical prediction.

The dynamical arrest in the liquid when $T \rightarrow T_g$, as implied by Fig. 10, is intuitively appealing. The observed continuous behaviour of the nematic-crystal transition upon freezing, and of the crystal-nematic transition upon melting, while both transitions are separated by a hysteresis, are indeed puzzling.

In an earlier parametrization of the data¹¹ we used the relation $\omega^2 \propto (\Delta T - \Delta T_c)^\gamma$, in analogy with equilibrium transition. We then showed that γ possibly could be ascribed to the Heisenberg universality class with dimensional cross-over. In that analysis we assumed a single transition ΔT_c . In the present analysis we have relaxed this condition and assumed a q -dependent ΔT_c , and the apparent cross-over behaviour is shown to be due to a shift to other Fourier modes. Perhaps it also indicates that the assumption of a single T_c for all harmonics of smectic order parameters¹⁸ is too rigid.

REFERENCES

1. P. Bergé and M. Dubois, *Cont. Phys.* **25**, 535 (1984).
2. M.J. Feigenbaum, *Phys. Lett.* **74A**, 375 (1979).
3. P. Pieranski, F. Brochard and E. Guyon, *J. de Physique* **33**, 681 (1972), *ibid.* **34**, 35 (1973).
4. H.N.W. Lekkerkerker, *J. Physique Lett.* **38**, L-277 (1977).
5. M.G. Velarde and I. Zuniga, *J. Physique*, **40**, 725 (1979).
6. E. Dubois-Violette and M. Gabay, *J. Physique* **43**, 1305 (1982).
7. E. Guyon, P. Pieranski and J. Salan, *J. Fluid Mech.* **93**, 65 (1979).
8. H.B. Möller and T. Riste, *Phys. Rev. Lett.* **34**, 996 (1975).
9. K. Otnes and T. Riste, *Phys. Rev. Lett.* **44**, 1490 (1980).
10. T. Riste and K. Otnes, *Phys. Scr.* **T9**, 76 (1985).
11. K. Otnes and T. Riste, *Phys. Scr.* **35**, 158 (1987).
12. T. Riste and K. Otnes, *Z. Phys. B - Condensed Matter* **68**, 265 (1987).
13. T. Riste and K. Otnes, *Z. Phys. B - Condensed Matter* (in press).
14. I. Catton, *Int. J. Heat Mass Transfer* **15**, 665 (1972).
15. F.H. Busse, *J. Fluid Mech.* **52**, 97 (1972).
16. F.H. Busse, *Rep. Progr. Phys.* **41**, 1929 (1978).
17. F. Heslot, B. Castaing and A. Libchaber, *Phys. Rev.* **36A**, 5870 (1987).
18. K. Otnes and T. Riste (unpublished).
19. R. Pynn, K. Otnes and T. Riste, *Solid State Comm.* **11**, 1365 (1972).
20. T. Riste and K. Otnes, *Physica* **137B**, 141 (1986).
21. O. Kvernøld, *Int. J. Heat Mass Transfer* **22**, 395 (1979).
22. J. Frøyland, *Proc. 11th IMACS World Congress*, Vol. 4, p. 281 (1985).
23. V.V. Beloshapkin, A.A. Chernikov, M. Ya. Natenzon, B.A. Petrovichev, R.Z. Sagdeev and G.M. Zaslavsky, *Nature* **337**, 133

- (1989).
24. S.M. Shapiro, J.D. Axe, G. Shirane and T. Riste, Phys. Rev. A 6, 4332 (1972).
 25. R.A. Cowley, J. Phys. Soc. Jpn., Suppl. 28, S239 (1970).
 26. W. Urbach, H. Hervet and R. Rondelez, Mol. Cryst. Liq. Cryst. 46, 209 (1978).
 27. A.C. Diogo and A.F. Martins, Mol. Cryst. Liq. Cryst. 66, 453 (1981).
 28. T. Riste and R. Pynn, Solid State Comm. 12, 409 (1973).
 29. J.D. Brock, R.J. Birgenau, J.D. Litster and A. Aharony, Physics Today 42, 52 (1989).